

## International Journal of Bio-Inorganic Hybrid Nanomaterials

# Influences of $\text{Co}^{2+}$ & $\text{Er}^{3+}$ Co-doping on the Structural and Physical Properties of ZnO Nanocrystals Synthesized by Hydrothermal Route

Saeideh Jannesarahmadi<sup>1\*</sup>, Abdolali Alemi<sup>2</sup>

<sup>1</sup> M.Sc., Department of Inorganic Chemistry, Faculty of Chemistry, University of Tabriz, Tabriz, Iran

<sup>2</sup> Professor, Department of Inorganic Chemistry, Faculty of Chemistry, University of Tabriz, Tabriz, Iran

Received: 3 August 2014; Accepted: 7 October 2014

### ABSTRACT

$\text{Co}^{2+}$  &  $\text{Er}^{3+}$  co-doped ZnO nanocrystals were synthesized by the hydrothermal method at 180°C and pH= 12 for 48 h. Powder XRD patterns indicate that the  $\text{Zn}_{1-2x}\text{Er}_x\text{Co}_x\text{O}$  crystals ( $0.00 < x \leq 0.035$ ) are isostructural with ZnO. The cell parameters increase for  $\text{Er}^{3+}$  and  $\text{Co}^{2+}$  upon increasing the dopant content (x). SEM images show that doping of  $\text{Er}^{3+}$  and  $\text{Co}^{2+}$  into the sites of  $\text{Zn}^{2+}$  does not change the morphology of ZnO. The FT-IR results indicate that the change in the peak position of ZnO absorption bands reflect that Zn-O-Zn network is perturbed by the presence of Er and Co in its environment. Semiconductor properties of these oxides are investigated by UV-Vis spectroscopy that there are red shifts as well as decreasing intensity of absorption peaks in doped nanomaterials.

**Keyword:** Co-doping; Nanocrystal; Erbium; Hydrothermal; Semiconductor; Cell Parameters.

## 1. INTRODUCTION

Zinc oxide has recently been the point of considerable attention due to its wide band gap (3.37 eV) and large free exciting band energy (60 meV). Zinc oxide in normal environmental conditions and thermodynamic equilibrium has the structure of hexagonal wurtzite, with lattice constants  $a = 3.2495 \text{ \AA}$  and  $c = 5.2069 \text{ \AA}$  [1, 2]. In such structure the ions of oxygen and zinc have coordination number 4 with opposing charges, which

occupy only 44% of volume of zinc oxide crystal. This void space thus created, is the source of defects in the ZnO. Doping methods have been extensively utilized for modifying the structures of ZnO nanoparticles to achieve new or improved chemical and physical properties [3-6]. Nano zinc oxide have so far been synthesized using methods such as hydrothermal [7], sol-gel [8], microwave [9], etc. and also doped systems by

(\*). Corresponding Author - e-mail: jannesar.saeideh@yahoo.com

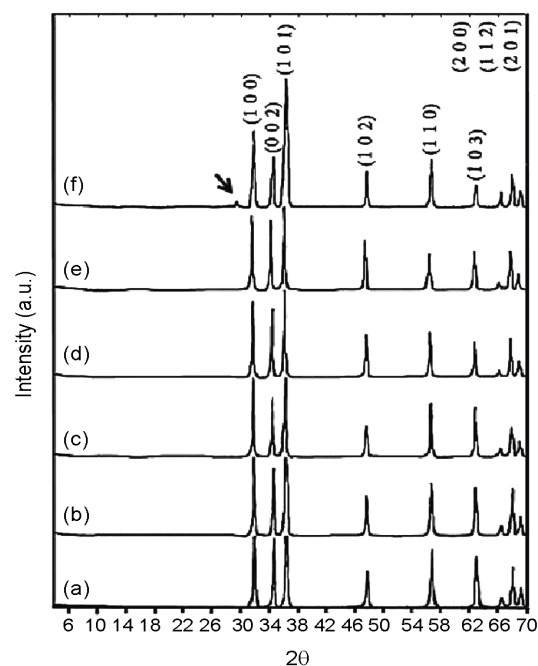
using many of the Lanthanides and transition metal. Nevertheless, so far, there is no report about co-doping of Lanthanides and transition cations into the lattice of ZnO. So, this paper maybe considered to be the first report on the subject.

## 2. MATERIALS AND METHODS

All chemicals were of analytical grade and used without further purification from Merck company.  $\text{Zn}(\text{NO}_3)_2 \cdot 6\text{H}_2\text{O}$ ,  $\text{Co}(\text{NO}_3)_2 \cdot 6\text{H}_2\text{O}$  and  $\text{Er}_2\text{O}_3$  were used as Zinc, Cobalt and Erbium sources, respectively. NaOH was used for alkalizing of reaction solution. ZnO powder with different  $\text{Co}^{2+}$  and  $\text{Er}^{3+}$  co-doping concentrations (0, 1, 2, 3, 3.5 and 4 mol%) were prepared by hydrothermal method. Usually,  $\text{Zn}(\text{NO}_3)_2 \cdot 6\text{H}_2\text{O}$ ,  $\text{Co}(\text{NO}_3)_2 \cdot 6\text{H}_2\text{O}$  and  $\text{Er}_2\text{O}_3$  were dissolved in distilled water to obtain 0.2 mol/L mix solutions. 20 mL of 2 mol/L sodium hydroxide solutions was slowly added into above-mentioned mix solution, stirred at room temperature for 30 min and then moved to a Teflon-lined stainless steel autoclave of 100 mL capacity. The autoclave was sealed, maintained at 180°C for 48 h and then cooled to room temperature. The green precipitate obtained was filtered and washed with ethanol and deionized water. It was dried at room temperature. Phase identification was performed with X-ray powder diffractometer (XRD D5000 Siemens) with Cu-K $\alpha$  radiation. The morphology of the materials was examined using a JEOL JSM6700F Scanning Electron Microscope. The Fourier transformed infrared (FT-IR) spectra for these samples were obtained using Tensor 27 spectrometer. The absorption spectra were recorded with UV-Vis spectrophotometer (Shimadzu 1700). Cell parameters were calculated with Cellref program from powder XRD patterns.

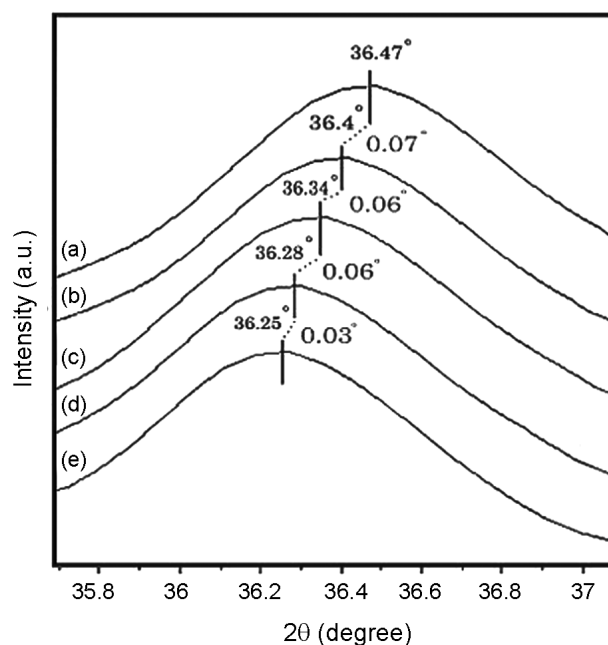
## 3. RESULTS AND DISCUSSION

Figure 1 shows the powder XRD patterns of the  $\text{Zn}_{1-2x}\text{Er}_x\text{Co}_x\text{O}$  nanoparticles with Co and Er co-doping concentrations of  $x = 0.00, 0.01, 0.02, 0.03, 0.035$  and  $0.04$ . These XRD patterns show that no other impurity phases exist for doping concentrations up to 3.5%.



**Figure 1:** Compared XRD patterns of (a) pure ZnO, (b)  $\text{Zn}_{0.98}\text{Er}_{0.01}\text{Co}_{0.01}\text{O}$ , (c)  $\text{Zn}_{0.96}\text{Er}_{0.02}\text{Co}_{0.02}\text{O}$ , (d)  $\text{Zn}_{0.94}\text{Er}_{0.03}\text{Co}_{0.03}\text{O}$ , (e)  $\text{Zn}_{0.93}\text{Er}_{0.035}\text{Co}_{0.035}\text{O}$ , (f)  $\text{Zn}_{0.92}\text{Er}_{0.04}\text{Co}_{0.04}\text{O}$ .

The Co and Er co-doping does not change wurtzite structure of ZnO. XRD pattern of  $\text{Zn}_{0.92}\text{Er}_{0.04}\text{Co}_{0.04}\text{O}$  sample displays a weak undesired peak at 29.31°, which corresponds to the (200) diffraction peak of  $\text{Er}_2\text{O}_3$ . In order to study the effect of Er and Co co-



**Figure 2:** High-resolution of (101) diffraction peak of  $\text{Zn}_{1-2x}\text{Er}_x\text{Co}_x\text{O}$ , (a)  $x = 0.00$ , (b)  $x = 0.01$ , (c)  $x = 0.02$ , (d)  $x = 0.03$ , (e)  $x = 0.035$ .

**Table 1:** Lattice constants (*a* and *c*) of  $Zn_{1-2x}Er_xCo_xO$ .

Samples	a (Å)	c (Å)
ZnO	3.2419	5.1908
$Zn_{0.98}Er_{0.01}Co_{0.01}O$	3.2467	5.1956
$Zn_{0.96}Er_{0.02}Co_{0.02}O$	3.247	5.1976
$Zn_{0.94}Er_{0.03}Co_{0.03}O$	3.2488	5.2005
$Zn_{0.93}Er_{0.035}Co_{0.035}O$	3.2499	5.2057

doping, a careful analysis of the position of the XRD peaks indicate that there is a shifting in peak's position towards lower  $2\theta$  value with increasing Er and Co contents (Figure 2).

The lattice parameters calculated from the XRD data demonstrate that their values increase with the increase of Er and Co co-doping (see Table 1). The two results above are understandable, because the effective ionic radius (0.881 Å) of  $Er^{3+}$  and (0.745 Å) of  $Co^{2+}$  in tetrahedral configuration is larger than  $Zn^{2+}$  (0.74 Å). Figure 3 shows the SEM images of 1% and 3.5% Er and Co co-doped ZnO nanoparticles which

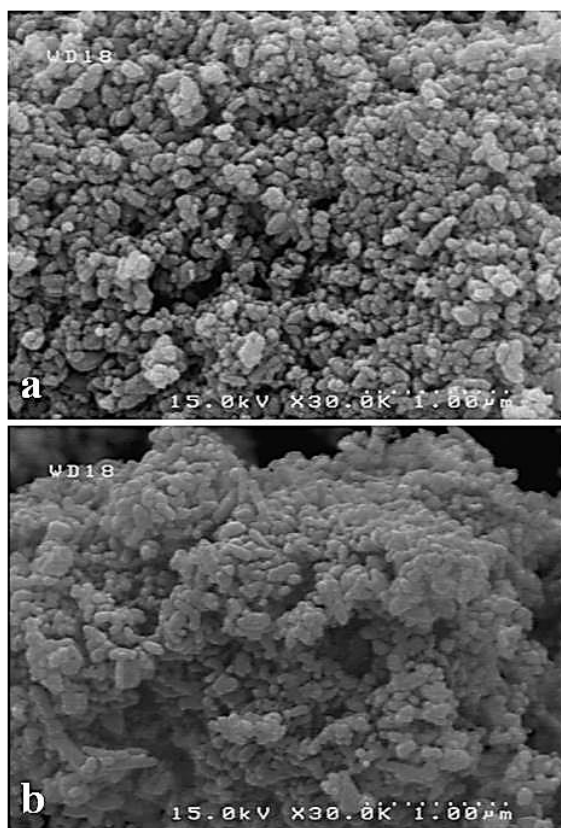


**Figure 3:** SEM images of  $Zn_{1-2x}Er_xCo_xO$  nanoparticles (a)  $x=0.01$  and (b)  $x=0.035$ .

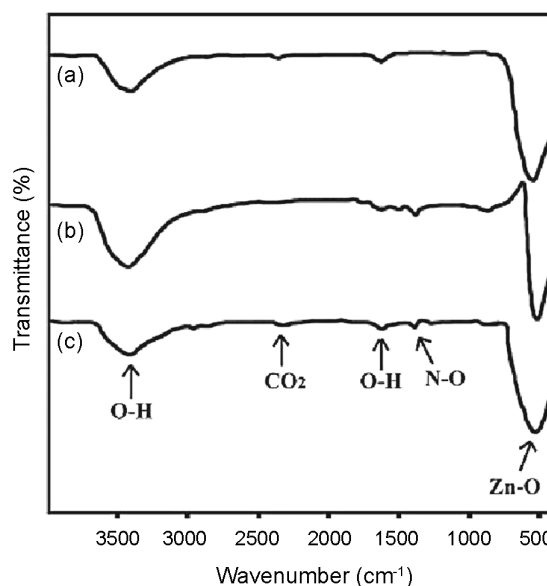


**Figure 4:** FT-IR spectra of  $Zn_{1-2x}Er_xCo_xO$  nanoparticles (a)  $x=0$  (b)  $x=0.01$  and (c)  $x=0.035$ .

are homogeneous and agglomerated. It is clear from the SEM images that the particles are nearly spherical in shape. In general, the average size of the particles augments with the increase of dopant content which varies from 55 nm for 1% to 65 nm for 3.5% Er and Co co-doped samples.

In addition, it is found that, the size of the particles become larger with the increase of  $Er^{3+}$  and  $Co^{2+}$  co-doping concentration. To study the change in Zn–O bonding due to the Er and Co substitution, FTIR measurements of Er and Co co-doped ZnO was carried out as shown in Figure 4. The FTIR spectra show main absorption bands near  $3400\text{ cm}^{-1}$  represent O–H mode, band arising from the absorption of atmospheric  $CO_2$  on the metallic cations at  $2350\text{ cm}^{-1}$ . The absorption band at  $542\text{ cm}^{-1}$  is the stretching mode of ZnO.

However, in case of 0%, 1% and 3.5% Co and Er co-doped samples, the value of absorption bands were found to be blue shifted at 542, 538 and  $530\text{ cm}^{-1}$ , respectively. The change in the peak position of ZnO absorption bands reflects that Zn–O–Zn network is perturbed by the presence of Er and Co in its environment. FTIR results also indicate that Er and Co is occupying Zn position in ZnO matrix as observed in the XRD measurements.

Semiconductor properties of the as-prepared ZnO nanostructure samples were revealed by UV–Vis

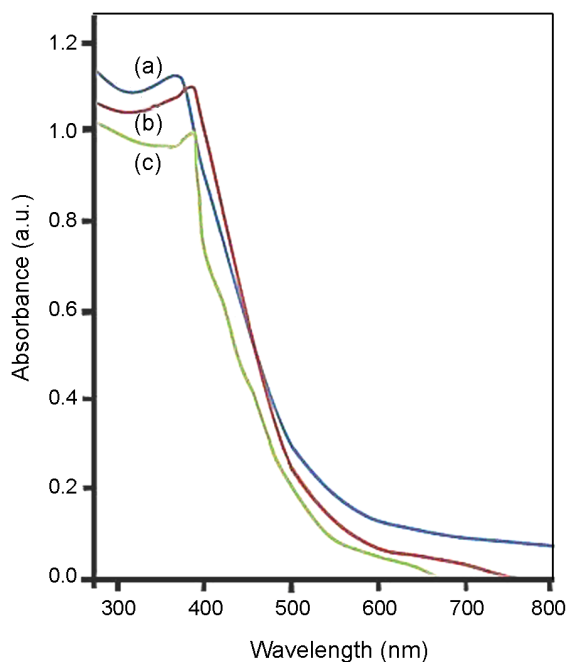


**Figure 5:** UV-Vis spectra of  $Zn_{1-2x}Er_xCo_xO$  nanoparticles (a)  $x=0$  (b)  $x=0.01$  and (c)  $x=0.035$ .

spectra, as shown in Figure 5.

The spectra portrays a characteristic absorption peaks of ZnO at wavelength of 350-400 nm which can be assigned to the intrinsic band-gap absorption of ZnO due to the electron transitions from the valence band to the conduction band ( $O_{2p} \rightarrow Zn_{4s}$ ). There are red shifts as well as decreasing intensity of absorption peaks in doped nanomaterials. The band gaps of undoped, 1% and 3.5% Co & Er co-doped ZnO are 3.32, 3.22 and 3.18 eV, respectively. As it is found, the band gap decreases while dopant content increases and it looks as though the increase in the diameter of the synthesized nanoparticles has been very likely a contributing factor.

#### 4. CONCLUSIONS

Nanoparticles of zinc oxide were purely synthesized

by hydrothermal method. XRD patterns confirm that  $Zn_{1-2x}Er_xCo_xO$  nanocrystals with dopant content,  $x$  of up-to 0.035 crystallize with wurtzite hexagonal structure. SEM images indeed indicate that no change in the morphology of ZnO has taken place as a result of doping. The red shift observed in the FT-IR spectrums are related to the perturbing in the ZnO matrix caused by  $Co^{2+}$  and  $Er^{3+}$  cations replacing the  $Zn^{2+}$ . UV-Vis spectra confirm that the band gap decreases with increase in the amount of dopant.

#### ACKNOWLEDGMENT

The authors are grateful to research council of the University of Tabriz for the financial support of this research.

#### REFERENCES

1. Baruah S., Dutta J., *Sci. Tech. Adv. Mater.*, **10** (2009), 188.
2. Look D.C., *Mater. Sci. Eng.*, **80** (2001), 383.
3. Chakraborty S., Kole A.K., Kumbhakar K., *Mater. Lett.*, **67** (2012), 362.
4. Yi G., Wang C., Park W., *Semicond. Sci. Technol.*, **20** (2005), 22.
5. Schmidt-Mende L., Judith L., *Mater. Today*, **10** (2007), 41.
6. Djurisic A.B., Ng A.M.C., Chen X.Y., *Prog. Quant. Electron*, **34** (2010), 191.
7. Ni Y., Wei X., Hong J., *Mater. Sci. Eng.*, **34** (2005), 121.
8. Shokouhfar A., Samei J., Vaezi M.R., Esmaeilzadeh A., *Def. Diff.*, **723** (2008), 626.
9. Rasouli S., Saket S., *Prog. Color Colorants Coat*, **3** (2010), 19.